THE USE OF A CLIMATE-TYPE CLASSIFICATION FOR ASSESSING CLIMATE CHANGE EFFECTS IN EUROPE FROM AN ENSEMBLE OF NINE REGIONAL CLIMATE MODELS

M. de Castro[(1)], C. Gallardo[(1)], K.Jylha[(2)] and H. Tuomenvirta[(2)]

(1) ICAM-UCLM, Toledo (Spain)

(2) FMI, Helsinki (Finland)

Summary

Making use of the Köppen-Trewartha (K-T) climate classification, we have found that a set of nine high-resolution regional climate models (RCM) are fairly capable of reproducing the current climate in Europe. The percentage of grid-point to grid-point coincidences between climate subtypes based on the control simulations and those of the Climate Research Unit (CRU) climatology varied between 73% and 82%. The best agreement with the CRU climatology corresponds to the RCM "ensemble mean". The K-T classification was then used to elucidate scenarios of climate change for 2071-2100 under the SRES A2 emission scenario. The percentage of land grid-points with unchanged K-T subtypes ranged from 41 to 49%, while those with a shift from the current climate subtypes towards warmer or drier ones ranged from 51 to 59%. As a first approximation, one may assume that in regions with a shift of two or more climate subtypes, ecosystems might be at risk. Excluding northern Scandinavia, such regions were projected to cover about 12% of the European land area.

1. Introduction

Two of the central concerns for the global change research today are to project the intensity and distribution of anthropogenic climate change in the future and to estimate the magnitude of its possible impacts on terrestrial ecosystems. For the first question, validated climate models are run making use of prescribed emission scenarios of greenhouse gases and aerosols. A possible, although highly approximate approach to achieving the second objective is the use of climate-vegetation classification schemes. In this study we try to address both issues by applying a climate classification scheme to the outcomes from nine high-resolution regional climate models in Europe.

Various global and regional climate models are currently used to quantify the climate response to present and future human activities. The first step in gaining confidence in the ability of climate models to produce reliable climate change projections is to evaluate their performance in reproducing the main processes in the climate system. The most widely-used procedure for verifying climate models consists of a systematic comparison between spatial distributions of observed and modelled annual, seasonal or monthly statistics of climate variables. See for example the Christensen and Kuhry (2000) and Achberger et al (2003) for RCM performance studies in some Northern European areas, and Jacob et al. (2006) for validation analyses of the models used in this study. Unfortunately, this requires a series of maps for each variable and period to be constructed and compared. An alternative way is to combine temperature and precipitation regimes on a single map, using a climate classification scheme. This simplifies the evaluation of climate models. The same classification scheme can also be utilized to elucidate the relative magnitude and spatial distribution of climate perturbations under various climate change scenarios. For example, in projected future climate scenarios, any projected temperature rise combined with a precipitation change in either direction can be rather easily translated into alterations in climate regimes and even, as discussed below, into zero-order estimates of potential impacts on terrestrial ecosystems. This kind of elucidation of climatic information would undoubtedly be quite useful for specialists in other scientific fields, for policy makers or even for the general public.

An important advantage in using the climate classification schemes is the easy association of each climate type with a vegetation class in present climate conditions (e.g., Table 1). This is founded on the fact that, although environmental and historical factors exert a decisive influence on the observed natural vegetation at the local scale (Leemans, 1992), climate acts as the main factor governing the broad-scale distribution of natural vegetation physiognomy and species composition. Indeed, the major patterns seen in many currently-used vegetation maps greatly resemble those of climate maps (see, e.g. Bartholomew et al., 1988).

Classifications for climate, vegetation and/or terrestrial ecosystems have been developed, cited here in chronological order, by Köppen (1936), Holdridge (1947), Thorthwaite (1948), Budyko (1986), Prentice et al. (1992) and Smith et al. (2002), among others. In the context of climate change, such classifications have been utilized by diverse authors. For example, Lohmann et al. (1993) used the Köppen climate classification for testing the ability of a global

model to reproduce current climate as well as for analysing how the large-scale climatic regions may alter under global warming scenarios. A modified Köppen classification was considered by Guetter and Kutzbach (1990) to analyse the impacts of changing climate on land cover patterns in past glacial and interglacial periods simulated by global climate model experiments. Projected future global biome redistribution caused by climatic change from four climate global models was analysed by Leemans et al. (1996) using various climate-vegetation classifications. Fraedrich et al. (2001) employed the Köppen scheme for the 1901--1995 period to examine continental climate shifts. Finally, Wang and Overland (2004) used the Köppen classification to detect Arctic climate change during the second half of the 20th century.

However, as often occurs when simple interpretation methods are applied, their advantages are unavoidably accompanied by some limitations. When climate classifications are used to assess the possible broad-scale impacts on vegetation of a projected climatic change, it must be kept in mind that: (a) There is uncertainty in the simulations of the future climate, (b) the relationships between climate and vegetation may not be the same in the future scenarios as in the current conditions, (c) the feedback of vegetation distribution changes on surface characteristics is ignored, and (d) climate-vegetation schemes only consider a few divisions which hardly represent the current vegetative diversity. Beside these, other relevant source of uncertainty is due to the fact that the regional models here used have been run under the constraint of the same global model, as stated by Dequé et al. (2005).

This article focuses on the use of a climate-vegetation scheme for analysing the ability of an ensemble of nine high-resolution regional climate models to reproduce current climate in Europe and for assessing the possible magnitude of climate change under a prescribed emission scenario for the last three decades of the 21st century. With the above mentioned limitations, the study may also be considered as a bulk approach to spotting the relative importance and distribution of the possible impact on European regional ecosystems of such a climate change scenario.

2. The Köppen-Trewartha climate classification

The first, and still the most widely-used, objective climate classification was developed by Köppen (1936), and was based on the concept that native vegetation is the best expression of climate. The strength of Köppen's climate classification is that it considers different latitudinal zones (based on extreme temperatures) and seasonality in both temperature and precipitation. Perhaps the main shortcoming of this classification, however, lies in the fact that the boundaries of certain climate types do not correspond with the observed boundaries of natural landscapes. This led G.T. Trewartha (Trewartha, 1968; Trewartha and Horn, 1980) to slightly modify the Köppen scheme by establishing more realistic criteria to distinguish between the B and C climate types and by adding a new major type (F). Table 1 shows the criteria used by the Köppen-Trewartha (hereafter K-T) climate classification, the equivalence of the K-T climate subtypes with those of the original Köppen scheme, and also the prevalent vegetation species within each K-T subtype which indicates the present-day correspondence between climate and natural landscapes.

We applied the K-T classification to European monthly mean temperature and precipitation data provided by the Climate Research Unit (CRU) of East Anglia University (New et al., 1999). This data base is available through the Internet web site *http://ipcc-ddc.cru.uea.ac.uk*. It contains climatological values on a 0.5º latitude/longitude grid over global land areas. The gridded values were obtained by applying a smooth fitting in 3-D space (latitude, longitude and elevation) to available surface observations at stations. For deducing the surface temperature at each grid-box height, a regionally and seasonally variable lapse rate was applied, which theoretically will give better results than other gridding methods which do not take elevation into account explicitly. The period of observation is 1961-1990 and the domain considered in this paper covers most of Europe (35N-75N, 15W-35E).

Figure 1a shows the resulting distribution of the K-T climate subtypes for the CRU climatology. All but four K-T subtypes (***FI, Cw, Aw, Ar***) are represented within the European land domain. The most abundant subtypes are ***Dc*** and ***Do***, both corresponding to temperate climates, and the former (latter) being the continental (oceanic) subtype prevalent in eastern (western) Europe. Subtropical climates (***Cs, Cr***) are limited to south of parallel 45N and sub-arctic or polar climates (***Eo, Ec, FT***) to north of parallel 60N approximately. The more elevated grid-boxes in the Alps region exhibit sub-artic climates because an alpine climate subtype is not considered in the K-T classification used.

3. The Regional Climate Models and the experiments

Within the European Union project known as PRUDENCE (after Prediction of Regional scenario and Uncertainties for Defining EuropeaN Climate change risks and Effects) a set of global and nested regional models has been applied for two of the IPCC-SRES emission scenarios (A2 and B2). The following analysis is concerned only with A2-based results from the regional models, all of them being nested with the same global model, as detailed below.

3.1 Regional climate models (RCM)

Nine state-of-the-art RCMs were used in the PRUDENCE project, with a common horizontal resolution of approximately 50 km. They are all finite difference, primitive equation hydrostatic models, but make use of different numerical schemes. All include essentially the same complete set of physical parameterisations, though individual schemes differ among the RCMs. This allows the RCM set to produce some variability in the response climate patterns, despite all of them using the same lateral conditions provided by a global climate model. A short description of the individual RCMs is found in Dequé et al. (2006); here only the acronyms and the research centre or institution of origin are given below for each model:

- The Danish Meteorological Institute (**DMI**) uses the HIRHAM model.
- The Met Office Hadley Centre (**HC**) uses the HadRM3H model.
- The Swiss Federal Institute of Technology (**ETH**) uses the CHRM model.
- The Geesthacht Institute for Coastal Research (**GKSS**) uses the CLM model.
- The International Centre for Theoretical Physics (**ICTP**) uses the RegCM2 model.
- Koninklijk Nederlands Meteorologisch Instituut (**KNMI**) uses the RACMO model.
- The Max-Planck Institute for Meteorology (**MPI**) uses the REMO model.
- The Swedish Meteorological and Hydrological Institute (**SMHI**) uses the RCAO model.
- The University Complutense of Madrid (**UCM**) uses the PROMES model.

Hereafter, each RCM will be referred to by the acronym of its respective centre or institution, instead of by the model name itself.

3.2 Climate simulations

All of the RCMs were run to simulate two 30-year time slices, one corresponding to the current climate (1961-1990) and the other to a climate change scenario (2071-2100). The radiative forcing for the future climate simulation corresponds to the IPCC SRES-A2 emission scenario (IPCC, 2000). Other details concerning the global model where all the RCM were nested, and the respective RCM domains and spatial resolutions (horizontal-vertical) can be found in Deque et al. (2006).

To evaluate and compare RCM results, all model outputs have been interpolated onto a common 0.5º x 0.5º grid identical to that of the CRU climatology. Those grid-points within the boundary relaxation zone of each RCM were excluded. Finally, analysis of the results has been restricted to land points in order to allow the evaluation of the RCM control experiments with CRU climatology and to comply with the secondary goal of the study concerning the qualitative effect of a climate change scenario on terrestrial ecosystems.

4. Results

4.1 Evaluation of RCM control runs

After determining the RCM-simulated 30-year averages of monthly mean 2-m temperature and precipitation totals for the control period (1961-1990), the K-T climate subtypes were calculated grid-point by grid-point for every RCM. Furthermore, using nine-model averages of monthly temperature and precipitation, a so-called "ensemble mean" distribution of climate subtypes was produced. For this calculation only the land grid-points common to all RCM were considered; these points numbered 3188. In addition, figure 1b also shows a wider domain common to at least 7 out of the 9 RCMs.

To quantify the point-to-point agreement between the RCM and the CRU, co-occurrence matrices were elaborated for each model. These co-occurrence matrices, given in Table 2, show the correspondences between the K-T climate subtypes from the CRU climatology and those from each RCM control simulation. The columns contain the number of land grid-points in each of the K-T subtypes according to the RCM control run (1961-1990) and the rows contain the numbers of each K-T subtype on the basis of the CRU climatology. Only the 3188 common land grid-points were included. For the interpretation of these matrices it should be

recalled that: (a) The main diagonal of each matrix indicates the number of land grid-points with coincident K-T subtypes between CRU and RCM; (b) the more spread the numbers are on both sides of the main diagonal, the less coincidence there is between climatology and model simulation; and (c) if the portion of cases below the main diagonal is larger than the portion of cases above, the corresponding RCM reference climate would be somewhat "warmer" than the CRU climatology (this is indeed the case for all RCMs).

Causes for the differences in K-T classification between CRU climatology and RCM-simulated 30-year averages can be divided into three parts. Firstly, simulated climate only approximates observed climate due to model simplifications, both in the RCMs and in the driving AGCM. Secondly, even a "perfect AGCM" forced with observed SSTs would not produce exactly the same climatology as observed, due to natural climatic variability. Thirdly, the accuracy of CRU climatology varies spatially, mostly due to the uneven distribution of observations (New et al., 1999).

The RCM simulations reproduce the CRU climatology fairly well, the percentage of point-to-point coincidences for the K-T subtypes varying between 73% and 82%. The largest differences between the CRU and the RCM control runs are found in the most abundant K-T subtypes: the temperate oceanic ***Do*** and the continental ***Dc***. The models simulated ***Do*** climates in a greater number of land grid-points than CRU climatology, while the number of grid-points for ***Dc*** was generally underestimated by the RCMs. This is clearly illustrated in figure 1b showing the RCM control "ensemble mean" distribution of K-T subtypes. The spatial arrangement of the "ensemble mean" simulated climate subtypes generally resembles the CRU pattern (figure 1a) quite closely in most of the domain, but the boundary between the ***Do*** and ***Dc*** climate subtypes crossing central Europe is displaced somewhat eastwards compared with the CRU. The eastward extension of the ***Do*** climate region seems to indicate that in winter the oceanic influence penetrates further inland in all of the RCM simulations, probably induced by the common driving AGCM, giving rise to a slight overestimation in the simulated average temperature of the coldest winter month, in comparison to the CRU climatology. Nevertheless, it must be borne in mind that the CRU gridded climatology itself may also contain some temperature bias, as Meier et al. (2004) reported for Scandinavia. This would introduce some uncertainty into the correct location of the boundaries between those K-T climate subtypes only differentiated by a sharp threshold in monthly mean temperatures, as is the case with ***Do*** and ***Dc***, and with ***Eo*** and ***Ec***.

Additional partial evaluation tests can be made for each RCM if co-occurrence matrices are analysed considering separately arid and subtropical subtypes (from ***BW*** to ***Cr***), limited to southern Europe and the Mediterranean regions, or sub-artic and polar subtypes (from ***Eo*** to ***FT***) located in the northernmost regions. For example, a secondary relative major disagreement between the RCM control runs and the CRU climatology relates to the portion of grid-points with ***BS*** subtype, which is slightly overestimated by most of RCMs. Taking into account the K-T classification criteria, this feature indicates an excess of modelled summer precipitation relative to winter rainfall, compared to the CRU climatology. Another evaluation analysis result comes from the spread into the ***Eo*** subtype column off the main diagonal seen in all the RCM results. This may again be related to a more extended oceanic influence in the model simulations with respect to the CRU climatology, as was mentioned in the ***Do*** subtype case.

A relevant result obtained in this comparative analysis is that the best agreement with CRU climatology is obtained by the RCM "ensemble mean", since it has the co-occurrence matrix with the largest portion of land grid-points in the main diagonal (82.5%). But the reason for this is not obvious. The number of grid-points covered by any subtype in the "ensemble mean" does not correspond to the arithmetic average of grid-point numbers from all of the RCMs for that subtype, because the K-T climate classification is a nonlinear process. Thus, the highest correspondence occurring between the "ensemble mean" and climatology is rather related to the higher reliability of simulated climates derived from a model ensemble compared with that of any individual member, probably because the averaging involved substantially reduces effects of natural (internal) variability and model-specific errors, as observed in multi-model studies of seasonal prediction (Doblas-Reyes et al., 2003). In this case, the multi-model average distributions of monthly mean temperature and precipitation, or actually their combination needed to obtain the K-T climate types, seem to be closer to reality than those produced by any individual model. This leads us to consider the advantage of using the RCM ensemble to elaborate more reliable projections of climate change and its possible impact on terrestrial ecosystems related to the K-T climate types, as is done in the next subsection.

4.2 Climate change scenario simulations

As mentioned above, the IPCC SRES-A2 emission scenario simulation for the last third of 21th century (2071-2100) was conducted by each of the RCMs nested in the HadAM3H global model. A description of projected changes in European temperature and precipitation simulated by the global model can be seen in Rowell (2005). In the regional climate experiments considered herein, each RCM explicitly calculates the effect of the prescribed greenhouse gases and sulphate aerosols evolution by means of particular specific parameterisations. The K-T climate subtypes for each land grid-point were then deduced from the 2m temperature and precipitation monthly averages calculated in the RCM scenario runs. For the sake of an easier visual assessment of the climate change, only the distribution of K-T subtypes derived from the nine-RCM "ensemble mean" of monthly temperature and precipitation is shown here (figure 2a). When this figure is compared to that of the control run (figure 1b), the more prominent, clearly-perceived features are: (a) A dramatic northeastward shift of the current central Europe boundary between the ***Do*** and ***Dc*** climate subtypes; (b) a penetration of the semiarid ***BS*** subtype into southern Spain, Italy and Greece; (c) a northward shift towards western France of subtropical climate types, even reaching into southern England; and (d) a northward shift of the subartic ***Eo*** subtype in Scandinavia.

For a quantitative assessment, the co-occurrence matrices expressing the point-by-point correspondence between K-T climate subtypes from the control and the A2 scenario runs in land areas of Europe are given in Table 3. The columns contain the counts of land grid-boxes in each of the K-T subtypes of the RCM scenario run (2071-2100), while the rows contain the counts for each K-T subtype of the same RCM control run (1961-1990). An easier understanding of the information that can be extracted from these matrices is achieved if we consider that: (a) The main diagonals designate the number of land grid-boxes with unchanged K-T subtypes; and (b) the numbers in each row on both sides of the main diagonal indicate the portion of grid-points that will undergo a change from the current climate subtype to that of the corresponding column in the projected climate change scenario.

The first result is that the portion of land grid-points with unchanged K-T subtypes ranges from 41 to 49%, and the portion of those with a shift from the current climate subtypes toward warmer or drier ones ranges from 51 to 59%. In just a few land grid-boxes in six RCMs there are surprising exceptions that suggest changes from a current ***Cs*** to a future ***Cr***. These are all due to an alteration in the proportion of winter/summer precipitation in the given RCM scenario run, rather than to an annual total rainfall increase. But the more significant changes

are to be found in the current climate ***Do, Dc*** and ***Ec*** subtypes (see Table 3). Pronounced increases (decreases) in the total regional coverage are simulated to take place for ***Do*** (***Dc*** and ***Ec***). Both the ***Do*** and ***Dc*** subtypes indicate a large spreading to the left of the main diagonal, corresponding in some grid-boxes to shifts even as far as the dry ***BS*** subtype. Also noticeable are the shifts of sub-artic ***Eo*** to temperate ***Dc*** and ***Do*** subtypes and those of ***Cs*** to the ***BS*** arid subtype or the more extreme changes in a few grid-points with a current ***BS*** climate to a ***BW*** desert subtype.

It is reasonable to deduce that many of these changes in K-T climate subtypes will result in alterations in terrestrial ecosystems in the future climate A2 scenario considered. Some of these changes could eventually even be as dramatic as to cause the disappearance of some vegetation species in certain European regions. Keeping in mind the cautions expressed in the Introduction concerning the limitations of the simple method used here, it may be considered that the most endangered European ecosystems would be those located in areas that experience a shift from the control to the A2 scenario of two or more climate subtypes, ranked as in the K-T classification. Taking only into consideration the more reliable results of the "ensemble mean", a total of 392 grid-points would experience such a "big" shift. Excluding northern Scandinavia and taking into account the variable grid-box sizes, these represent more than 12% of the European land area. Most of this "threatened" area is found in the Iberian Peninsula and western France, also marginally in southern England and at the mouth of the Danube valley (see figures 1b and 2a). Some RCMs even simulate the extremely dry ***BS*** climate subtype (actually desert) in some land grid-boxes (see Table 3). This is reflected too in the "ensemble mean" that is considered more reliable; in this, a few desert grid-boxes resulted over the SE of Spain (figure 2a). Also the few grid-points with current climate ***FT*** subtypes in the Alps shift to temperate ***Dc***, which could be a hint of glacier disappearance (or a drastic reduction at least) in the simulated A2 scenario. Although based on simulations with only 7 RCMs, it seems that some ecosystems in Northern Fennoscandia may experience large changes as ***FT*** [***Ec***] climate types are replaced with ***Eo*** [***Dc***] types.

Finally, we have compared the projected "ensemble mean" future K-T subtype distribution with that obtained using the so-called delta-change method. This method, frequently applied by climate change impact researchers, consists of adding simulated changes in climate, e.g., in monthly temperature and precipitation, to current climatology. To enable the comparison, the averages of the monthly changes between scenario and control runs in the nine RCMs were

first calculated for each common land grid-points. These “delta” values were then added to the corresponding gridded 30-year (1961-1990) average monthly temperature and precipitation of the CRU climatology. Using these “perturbed” monthly temperature and precipitation values the K-T subtypes were then deduced (figure 2b).

Figures 2a and 2b facilitate a visual comparison between the scenario K-T climate subtype distributions that result directly from climate change RCM simulations and the corresponding distribution obtained from the “delta method”. The main features in both figures are quite similar, though the K-T- climate subtype shifts are in general a bit less severe in the “delta method”. In the model “ensemble mean” method the percentage of land grid-points that experience a K-T subtype change is 56%, while in the “delta method” this number is only 47%. More noticeable differences between both methods appear, however, when looking at regional details, as for example on the Iberian Peninsula or in western France. Most surprisingly, in these regions there are no major differences in the K-T classification between the CRU climatology and “ensemble mean” control experiment (see figures 1a and 1b). Therefore, the regional-scale differences between climatology and the current climate simulation are not translated into climate change scenario consequences in a straightforward manner. The goal of this comparison was not to discriminate between the respective adequacy or reliability of the various methods, but to point out that they might not give the same results if applied to impact studies on a regional or local scale.

5. Concluding remarks

The Köppen-Trewartha climate classification has been used for analysing the ability of nine high-resolution regional climate models (RCM) to reproduce the current climate type distribution over Europe and for assessing how it would be altered under a simulated climate change scenario. Two 30-year time-slice simulations were carried out by each RCM: the 1961-1990 period, i.e., a control simulation of the "present" climate and of the 2071-2100 period, i.e., a scenario simulation of future climate (SRES-A2). All of the RCMs were forced with the same boundary conditions provided by one global atmospheric model.

The RCM control runs reproduced the K-T climate subtype distribution deduced from a gridded climatology (CRU] fairly well. Point-by-point coincidences ranged from 73% to 82% out of a total of 3188 land grid-points covering most of Europe. The highest correspondence

(close to 83%) was obtained, however, when the 9-RCM ensemble monthly temperature and precipitation mean values were used for deducing the K-T climate types. This result leads us to conclude that an RCM ensemble might offer more reliable projections of climate change than any individual member.

Results from the climate change scenario run produce a noteworthy alteration in the current K-T climate subtypes distribution over Europe. It consists essentially of a deep inland penetration of the temperate oceanic subtype (Do) across central Europe, an enlargement of areas with the semiarid BS subtype in southern Mediterranean regions, and a northward shift of the subtropical climate subtypes reaching western France and into southern England, as well as a corresponding shift of the oceanic sub-artic Eo subtype in Scandinavia.

Speculations can be made about the impact of such alterations in the actual K-T climate type distribution on terrestrial ecosystems for the future scenario considered, given the close correspondence between the climate classification used and prevalent vegetation species. The greatest climate subtype changes might be dramatic enough to cause the disappearance of at least the most endangered ecosystems in certain European regions. Considering a subjective, though reasonable, criterium, the most threatened areas in Europe could represent more than 12% of its total surface, this being mostly concentrated in the Iberian Peninsula, western France, southern England, the easternmost part of the Danube valley, and probably also northern parts of Fennoscandia. However, this conclusion must be understood as a first approach to the intensity of the possible impact on European ecosystems in a climate change scenario, given the limitations of the simple method applied, as commented on in section 1.

Finally, the future climate K-T subtype distribution was deduced by applying the delta method, consisting of adding simulated changes in monthly temperature and precipitation to the gridded actual climatology (CRU). This distribution has been compared to that obtained directly from the projected RCM ensemble mean. The conclusion to be drawn is that the two methods do not give the same K-T distribution in a future climate. This reminds us of the fact that regional or local-scale impact studies using the delta method, as is frequently the case, do not necessarily give the same results as impact models forced directly with RCM output.

Acknowledgments

The work reported herein was carried out under the European Commission Programme Energy, Environment and Sustainable Development contract EVK2-2001-00156 (PRUDENCE project). The Spanish contribution was partly supported by the MCYT contract REN2000-0769 (GERCLIMPE project). A thorough reading of the manuscript and comments from two referees are appreciated.

References

Achberger, C., M.-L. Linderson and D. Chen (2003): Performance of the Rossby Centre regional atmospheric model in Southern Sweden: comparison of simulated and observed. *Theor. Appl. Climatol*., 76, 219-234

Bartholomew, J.C., J.H. Christie, A. Ewington, P.J.M. Geelan, H.A.G. Lewisobe, P. Middketon and H. Winkleman Eds) (1988): *The Times' Atlas of the World*. Times Books Limited, London.

Budyko, M.I. (1986): *The Evolution of the Biosfere*. D. Reidel Publ. Co., Dordrecht.

Christensen, J.H. and P. Kuhry (2000): High-resolution regional climate model validation and permafrost simulation for the East European Russian Artic. *J. Geophys. Res.*, 105(D24), 29647-29658.

Dequé, M., D.P.Rowell, D. Lüthi, F.Giorgi, J.H.Christensen, B.Rockel, D.Jacob, E. Kjellström, M.de Castro and B.van den Hurk (2005): An intercomparison of regional climate simulations for Europe: assessing uncertainties in model projections. Accepted in *Clim. Change* Special Issue on the PRUDENCE project.

Doblas-Reyes, F., V. Pavan and D Stephenson. The skill of multi-model seasonal forecasts of the wintertime nao. *Clim. Dyn*., 21, 501-514.

Fraedrich, K., F.-W. Gerstengarbe, P.C. Werner (2001): Climate shifts during the last century. *Clim. Change*, 50, 405-417.

Holdridge, L.R. (1947): Determination of world formations from simple climatic data, *Science,* 105, 367- 368.

Jacob, D., L. Bärring , O. B. Christensen , J. H. Christensen, M. de Castro, M. Déqué, F. Giorgi, S. Hagemann, M.Hirschi, R. Jones, E. Kjellström, G. Lenderink, B.Rockel, E. Sánchez, C. Schär, S. I. Seneviratne, S. Somot, A.van Ulden, B. van den Hurk (2005): An inter-comparison of regional climate models for Europe:Design of the experiments and model performance. Accepted in *Clim. Change* Special Issue on the PRUDENCE project.

Köppen, W. (1936): “Das Geographische System der Klimate”. In Köppen and Geiger (eds) *Handbuch der Klimatologie*, Vol I, Part C, Gebrüder Borntraeger, Berlin.

Leemans, R. 1992): Modelling ecological and agricultural impacts of global change on a global scale. *J. Sci. Ind. Res*., 51, 709-724.

Leemans, R., W. Cramer and J.G. Van Minnen (1996): Prediction of global Biome distribution using bioclimatic equilibrium models, in Breymeyer et al. (eds) *SCOPE56-Global Change: Effects on Coniferous Forests and Grasslands*, J. Wiley, New York.

Lohmann, U., R. Sausen, L. Bengtsson, U. Cubasch, J. Perlwitz and E. Roeckner (1993): The Köppen climate classification as a diagnostic tool for general circulation models. *Clim. Res*., 3, 177-193.

IPCC (2000) : *Emissions Scenarios. A Special Report of Working Group III of the Intergovernmental Panel on Climate Change*. Cambridge University Press, 599 pp.

Meier, H.E.M., R. Doscher and A. Halkka (2004): Simulated distributions of Baltic Sea-ice in warming climate and consequences for the winter habitat of the Baltic ringed seal. *Ambio* 33, 249-256.

New, M., M. Hulme and P. Jones (1999): Representing twentieth-century space-time climate variability. Part I: Development of a 1961-90 mean monthly terrestrial climatology. *J. Climate*, 12, 829-856.

Prentice, J.C., W. Cramer, S.P. Harrison, R. Leemans, R.A. Monserud and A.M. Solomon (1992): A global biome model based on plant physiology and dominance, soil properties and climate. *J. Biogeogr*., 19, 117- 134.

Rowell, D.P. (2005): A scenario of European climate change for the late 21st century: seasonal means and interannual variability. *Clim. Dyn.*, 25, 837-849.

Smith, G.L., A.C. Wilber, S.K. Gupta and P.W. Stackhouse (2002): Surface Radiation budget and climate classification. *J. Climate*, 15, 1175-1188.

Thorthwaite, C.W. (1948): An approach toward a rational classification of climate. *Geogr. Rev*., 38, 55-94.

Trewartha, G.T. (1968): *An Introduction to Climate*, McGraw-Hill, New York, 395-399

Trewartha, G.T. and L.H. Horn (1980): *An Introduction to Climate*, 5th Ed., McGraw Hill, New York.

Wang, M. and J.E. Overland (2004): Detecting Arctic climate change using Köppen climate classification. *Clim. Change*, 67, 43-62.

Climate	K - T	Köppen	Prevalent native vegetation type
Tropical humid	Ar	Af	Rain forest
Tropical wet-dry	Aw	Aw, As	Savanna
Dry arid	BW	BW	Desert
Dry semiarid	BS	BS	Steppe
Subtropical summer-dry	Cs	Cs	Hardleaved evergreen trees and shrubs
Subtropical summer-wet	Cw	Cw	Woodland patches, shrubs and prairies
Subtropical humid	Cr	Cf	Longleaf trees, slash pines and deciduous forest in inland areas
Temperate oceanic	Do	Cf, Cw	Dense coniferous forests with large trees
Temperate continental	Dc	Df, Dw, Ds	Needleleaf and deciduous tall broadleaf forest
Sub-arctic oceanic	Eo	Df, Dw, Ds	Needleleaf forest
Sub-arctic continental	Ec	Df, Dw, Ds	Tayga
Tundra	FT	ET	Tundra
Ice cap	FI	EF	Permanent ice cover

Note: Definitions of the Köppen–Trewartha climate types:

Ar: All months above 18ºC and less than 3 dry months (1).
Aw: Same as Ar, but 3 or more dry months.
BW: Annual precipitation P (in cm) smaller or equal than 0.5 · A (2).
BS: Annual precipitation P (in cm) greater than 0.5 · A.
Cs: 8 - 12 months above 10ºC, annual rainfall less than 89 cm and dry summer (3)
Cw: Same thermal criteria as Cs, but dry winter (4)
Cr: Same as Cw, with no dry season.
Do: 4–7 months above 10ºC and coldest month above 0ºC
Dc: 4–7 months above 10ºC and coldest month below 0ºC
Eo: Up to 3 months above 10ºC and temperature of the coldest month above –10ºC
Ec: Up to 3 months above 10ºC and the coldest month below or equal to –10ºC
Ft: All months below 10ºC
Fi: All months below 0ºC

(1) Dry month: Less than 6 cm monthly precipitation
(2) $A = 2.3\ T - 0.64\ Pw + 41$, being T the mean annual temperature (in ºC) and Pw the percentage of annual precipitation occurring in the coolest six months.
(3) Dry summer: The driest summer month less than 3 cm precipitation and less than one-third of the amount in the wettest winter month
(4) Dry winter: Precipitation in the wettest summer month higher than 10 times that of the driest winter month

Table 1. The Köppen-Trewartha (K-T) climate classification, equivalence between K-T climate subtypes and Köppen classification, and their correspondence with natural landscapes (from US Forest Service: *www.nearctica.com/ecology/ecoreg/append1.htm*).

"Ensemble mean"

CRU climatology	BW	BS	Cs	Cr	Do	Dc	Eo	Ec	FT
BW	0								
BS		9	1		1	1			
Cs		26	333	23	27				
Cr			22	39	9				
Do		3	10	30	890	16	2		
Dc			1		321	1243	26		
Eo					3	11	105		
Ec						1	16	0	
FT							8		11

tot = 3188 ; dg = 2630 ; ab = 106 ; be = 452

DMI

CRU climatology	BW	BS	Cs	Cr	Do	Dc	Eo	Ec	FT
BW	0								
BS	1	8	1	1	1				
Cs		102	242	45	20				
Cr		3	24	33	10				
Do		21	17	56	843	7	7		
Dc		39	5		306	1217	24		
Eo					2	17	96		4
Ec						5	12	0	
FT							7		12

tot = 3188 ; dg = 2451 ; ab = 120 ; be = 617

ETH

CRU climatology	BW	BS	Cs	Cr	Do	Dc	Eo	Ec	FT
BW	0								
BS	4	5	1		1	1			
Cs	6	97	223	10	73				
Cr		2	30	16	22				
Do		28	29	12	842	26	14		
Dc		3	2		225	1186	174	1	
Eo					2		110		7
Ec							14	1	2
FT							3		16

tot = 3188 ; dg = 2399 ; ab = 332 ; be = 457

GKSS

CRU climatology	BW	BS	Cs	Cr	Do	Dc	Eo	Ec	FT
BW	0								
BS		1	7		3	1			
Cs		1	212	125	71				
Cr			4	49	17				
Do			4	36	870	36	5		
Dc			2		344	1158	87		
Eo					2	5	108		4
Ec							16	0	1
FT							2		17

tot = 3188 ; dg = 2415 ; ab = 357 ; be = 416

HC

CRU climatology	BW	BS	Cs	Cr	Do	Dc	Eo	Ec	FT
BW	0								
BS	1	6		3	1	1			
Cs		58	264	41	46				
Cr		1	17	31	21				
Do		6	14	40	823	61	7		
Dc		1	1		267	1283	31	8	
Eo					2	2	113		2
Ec						2	12	3	
FT							8		11

tot = 3188 ; dg = 2534 ; ab = 222 ; be = 432

ICTP

CRU climatology	BW	BS	Cs	Cr	Do	Dc	Eo	Ec	FT
BW	0								
BS		6	2	1	2	1			
Cs	1	55	278	33	42				
Cr			24	33	13				
Do			13	24	871	39	4		
Dc					257	1301	33		
Eo					5	11	102		1
Ec							17	0	
FT							15		4

tot = 3188 ; dg = 2595 ; ab = 171 ; be = 422

KNMI

CRU climatology	BW	BS	Cs	Cr	Do	Dc	Eo	Ec	FT
BW	0								
BS	4	6			1	1			
Cs	3	128	247	5	26				
Cr	1	11	36	16	6				
Do	2	29	25	24	860	11			
Dc		37	1		370	1174	9		
Eo					10	34	75		
Ec						5	12	0	
FT							13		6

tot = 3188 ; dg = 2384 ; ab = 59 ; be = 745

MPI

CRU climatology	BW	BS	Cs	Cr	Do	Dc	Eo	Ec	FT
BW	0								
BS		8	3		1				
Cs	2	50	282	75					
Cr		1	23	45	1				
Do		14	31	97	807	2			
Dc			8		399	1182	2		
Eo					8	34	77		
Ec						5	12	0	
FT							16		3

tot = 3188 ; dg = 2404 ; ab = 84 ; be = 700

SMHI

CRU climatology	BW	BS	Cs	Cr	Do	Dc	Eo	Ec	FT
BW	0								
BS	3	6	2		1				
Cs	10	134	254	6	5				
Cr		4	50	12	4				
Do		2	73	31	842	3			
Dc		7	5		430	1139	10		
Eo					7	29	81		2
Ec						5	12	0	
FT							13		6

tot = 3188 ; dg = 2340 ; ab = 33 ; be = 815

UCM

CRU climatology	BW	BS	Cs	Cr	Do	Dc	Eo	Ec	FT
BW	0								
BS	1	8	1		1	1			
Cs	2	61	271	38	37				
Cr		3	15	45	7				
Do		18	3	32	868	23	7		
Dc					348	1128	115		
Eo					2	5	105		7
Ec							13	3	1
FT							1		18

tot = 3188 ; dg = 2446 ; ab = 238 ; be = 504

Table 2. Co-occurrence matrices from the CRU climatology to each of the RCM control simulations (1961-1990) and to the "ensemble mean" (see text for its meaning). Values denote the number of grid-points which are of subtype *i* in CRU but of type *j* in RCM. At the bottom of each table are given the total number of land grid-points in the common domain (tot), the portion of the matrix elements in the main diagonal (dg) and those above (ab) and below (be) the main diagonal.

"Ensemble mean" SRES-A2

ENS control	BW	BS	Cs	Cr	Do	Dc	Eo	Ec	FT
BW	0								
BS	8	30							
Cs		138	229						
Cr		6	56	30					
Do		48	259	144	800				
Dc		23			928	321			
Eo					45	106	6		
Ec								0	
FT						4	7		0

tot = 3188 ; dg = 1416 ; ab = 0 ; be = 1772

DMI SRES-A2

DMI control	BW	BS	Cs	Cr	Do	Dc	Eo	Ec	FT
BW	1								
BS	23	150							
Cs		112	174	3					
Cr		32	35	68					
Do		70	212	220	680				
Dc		50	1		878	317			
Eo					32	111	3		
Ec								0	
FT						5	11		0

tot = 3188 ; dg = 1393 ; ab = 3 ; be = 1792

ETH SRES-A2

ETH control	BW	BS	Cs	Cr	Do	Dc	Eo	Ec	FT
BW	10								
BS	49	86							
Cs	1	97	186	1					
Cr			11	27					
Do		80	172	37	876				
Dc		77			782	354			
Eo					73	217	25		
Ec						2		0	
FT						3	22		0

tot = 3188 ; dg = 1564 ; ab = 1 ; be = 1623

GKSS SRES-A2

GKSS control	BW	BS	Cs	Cr	Do	Dc	Eo	Ec	FT
BW	0								
BS		2							
Cs		37	185	7					
Cr		2	47	161					
Do		20	157	236	894				
Dc					948	252			
Eo					72	129	17		
Ec								0	
FT						1	21		0

tot = 3188 ; dg = 1511 ; ab = 7 ; be = 1670

HC SRES-A2

HC control	BW	BS	Cs	Cr	Do	Dc	Eo	Ec	FT
BW	1								
BS	20	52							
Cs		114	182						
Cr		31	44	40					
Do		54	252	160	694				
Dc		43	11	15	954	326			
Eo					35	132	4		
Ec						11		0	
FT						6	7		0

tot = 3188 ; dg = 1299 ; ab = 0 ; be = 1889

ICTP SRES-A2

ICTP control	BW	BS	Cs	Cr	Do	Dc	Eo	Ec	FT
BW	1								
BS	9	52							
Cs		122	195						
Cr		2	42	47					
Do		32	190	207	761				
Dc					963	389			
Eo					50	110	11		
Ec								0	
FT						1	4		0

tot = 3188 ; dg = 1456 ; ab = 0 ; be = 1732

KNMI SRES-A2

KNMI control	BW	BS	Cs	Cr	Do	Dc	Eo	Ec	FT
BW	10								
BS	61	150							
Cs		168	141						
Cr		2	28	15					
Do		66	257	134	816				
Dc		54	1		900	270			
Eo					29	77	3		
Ec								0	
FT						1	5		0

tot = 3188 ; dg = 1405 ; ab = 0 ; be = 1783

MPI SRES-A2

MPI control	BW	BS	Cs	Cr	Do	Dc	Eo	Ec	FT
BW	2								
BS	16	57							
Cs		96	241	10					
Cr		24	59	134					
Do		64	151	396	605				
Dc		10		14	898	301			
Eo					23	83	1		
Ec								0	
FT							3		0

tot = 3188 ; dg = 1341 ; ab = 10 ; be = 1837

SMHI SRES-A2

SMHI control	BW	BS	Cs	Cr	Do	Dc	Eo	Ec	FT
BW	13								
BS	44	108	1						
Cs		172	212						
Cr			24	25					
Do		68	364	164	693				
Dc		4			866	306			
Eo					38	75	3		
Ec								0	
FT						1	7		0

tot = 3188 ; dg = 1360 ; ab = 1 ; be = 1827

UCM SRES-A2

UCM control	BW	BS	Cs	Cr	Do	Dc	Eo	Ec	FT
BW	3								
BS	26	62	2						
Cs		102	188						
Cr		10	62	43					
Do		75	154	168	866				
Dc		58			793	306			
Eo					85	147	9		
Ec						3		0	
FT						9	17		0

tot = 3188 ; dg = 1477 ; ab = 2 ; be = 1709

Table 3. Co-occurrence matrices from the RCM control simulations (1961-1990) to the RCM A2 scenario run (2071-2100). Values denote the number of grid-points which are of subtype *i* in the control but of type *j* in the scenario run. At the bottom of each table are given the total number of land grid-points in the common domain (tot), the portion of the matrix elements in the main diagonal (dg) and those above (ab) and below (be) the main diagonal.

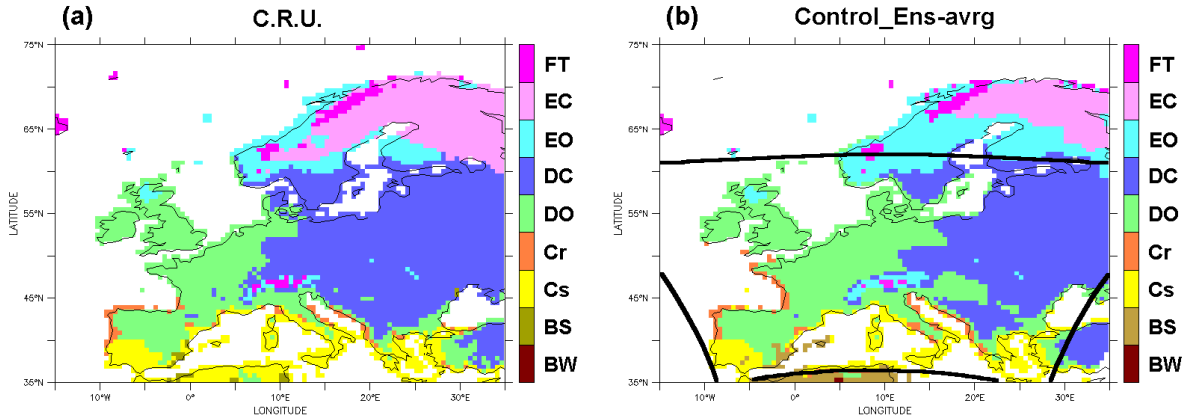

Figure 1. Köppen-Trewartha climate subtypes distributions deduced from: (a) The CRU climatology (1961-1990), and (b) the "ensemble mean" of the 9 RCM's control runs (1961-1990). The results outside the line frame are based on only 7-8 RCMs.

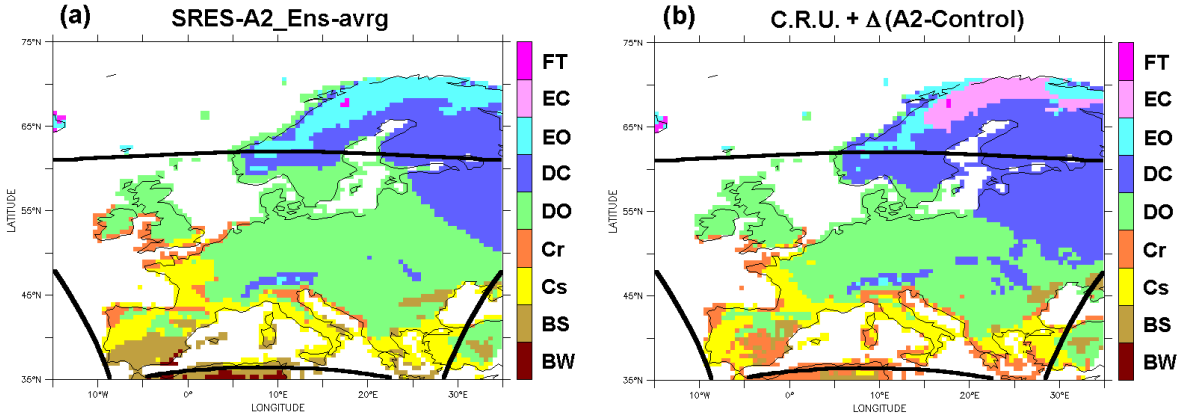

Figure 2. Köppen-Trewartha climate subtypes distributions deduced from: (a) The "ensemble mean" of the 9 RCM's A2 scenario runs (2071-2100) and (b) the CRU climatology plus the average climate change from the 9 RCMs obtained in the A2 scenario (2071-2100). The results outside the line frame are based on only 7-8 RCMs.